Tribology Letters, Vol. 26, No. 2, May 2007 (© 2007)
DOI: 10.1007/s11249-006-9188-3

Experimental and numerical investigations on development of cavitation erosion pits on solid surface

Chen Haosheng*, Li Yongjian, Chen Darong and Wang Jiadao

State Key Laboratory of Tribology, Tsinghua University, Beijing, 100084, China

Received 13 August 2006; accepted 1 December 2006; published online 9 January 2007

Polished, grinded, and milled samples made of 40Cr stainless steel were prepared for the cavitation erosion experiment. A typical phenomenon of "pits chain", which consisted of two contact pits and a smaller pit on the ridge between them, was found on the sample surfaces after 15-minute experiment. Numerical simulation indicated that the pressure fluctuation caused by the sequentially formed pits on the solid surface was the main reason for the formation of the "pits chain". It proves that the early-formed pits affect the formation of the subsequent erosion pits, and the whole cavitation erosion process is not a probability event. Based on the numerical analyses, the development of erosion is divided into four stages, which describe how a pit develops vertically and horizontally under the effect of the pressure perturbation. The development was validated by the characteristics of the damaged surface observed at different experimental time.

KEY WORDS: cavitation erosion, cavitation, wear, surface roughness

1. Introduction

Cavitation erosion is considered as the main reason for the damage of hydromachine surfaces in some conditions where abrasion and corrosion have little effect [1]. Usually, cavitation erosion level is represented by the mass loss curve, which can characterize different stages of the cavitation erosion [1]. However, the erosion developments and the surface characteristics in different erosion stages cannot be found from the mass loss curve. Whereas, erosion pits are obvious characteristics on the surface and their development can describe the erosion process [2–5]. In fact, they have already been used to describe the erosion process in the work done by Marques [4] and Yoshiro [5].

An erosion is commonly recognized as the result of the collapse of a bubble near a solid wall [1]. It has been proved that the pressure perturbation will break the stability of a spherical bubble, and then cause it to collapse [6]. On the other hand, experiment results have shown that cavitation erosion is easy to generate on a rough or wavy surface [7, 8]. The asperity and concave geometry of the surface are believed to cause the pressure perturbation and induce the bubble collapse. In real working conditions, bubbles may collapse near the machined surfaces, such as polished or grinded surfaces. When the pits are initially formed on such surfaces, the surface profile is changed. The changed surface profile causes the pressure fluctuation, which subsequently affects the formation of erosion pits. It is deduced that the cavitation erosion process is not a probability event; the development of the erosion pits obeys some rules.

In the undergoing study, three machining methods, polishing, grinding, and milling, were used to process samples made of stainless steel. The processed samples were used in the cavitation damage experiment. After different experimental time, the samples' surfaces were observed under a Scanning Electronic Microscope (SEM) to study the variation of the pits' number and shape. Later, numerical analyses are given to explain the characteristics of the damaged surfaces and the development of the pits.

2. Experimental section

2.1. Experimental apparatus

Figure1 shows a schematic of the rotating-disk cavitation apparatus. The diameter of the rotating-disk was 300 mm and four equispaced samples were installed on the rotating disk. To induce the cavitation, an orifice hole was made on the rotating-disk in front of each sample. The rotating speed of the rotating disk was 2,800 round/min, and the corresponding velocity of the samples was 30 m/s. In this experiment, the size of the sample was $40 \times 30 \times 6$ mm^3. As the sample installation site was 5 mm deep, the upper surface of the sample was 1 mm higher than the rotating disk surface. The fluid used in the experiment was tap water, and the temperature of the water in the

*To whom correspondence should be addressed.
E-mail: chenhs@mail.tsinghua.edu.cn

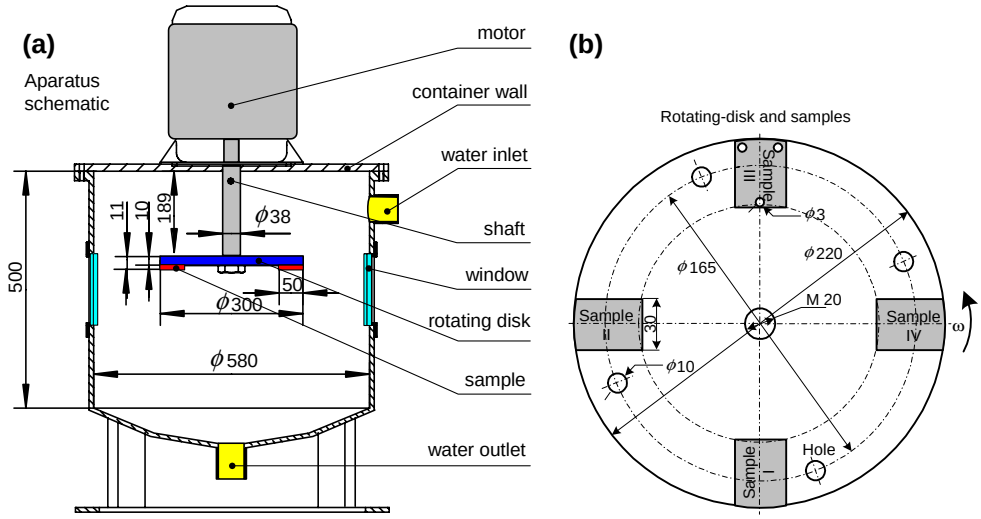

Figure 1. (a) Schematics of the cavitation experimental apparatus and (b) the installment of the samples.

Table 1.
Surface roughness and contact angles of different surfaces.

Process method	Milling	Grinding	Polishing
R_q (μm)	1.02	0.32	0.041
Contact angle (°)	96.63	84.05	75.17

experiment was kept at 25 °C by a water refrigerating circuit system HW-50.

2.2. Sample surfaces

In this experiment, the samples were made of 40Cr stainless steel, and their surfaces were processed by three methods: milling, grinding, and polishing. The surface roughness and the contact angle of each sample surface are listed in Table 1. The roughness is represented by the Root Mean Square (R_q). The milled and grinded surfaces were measured by the surface topography tester named Taylor Surf 120P, while the polished surface was measured by the Scanning Probe Microscope (SPM) named CSPM-4000, because the polished surface is too smooth to be measured by the surface topography tester. Besides the surface roughness, the wettability of the surface also has some effect on the cavitation erosion results [9]. Therefore, the contact angles of water were tested on different surfaces, and the results are listed in Table 1.

2.3. Experimental results

Three samples with different surfaces were installed on the rotating disk at the same time, and an unprocessed sample was also installed as a balance weight. The cavitation erosion experiment lasted 15 min. Such short experimental time is scheduled to reduce other damage effects on the surfaces, such as corrosion and abrasion. After the experiment, the samples were cleaned and observed. Besides the typical erosion pits commonly appearing on the surfaces in the cavitation experiment, a special erosion phenomenon was found, as shown in figure 2. The magnitude, scale, and other testing parameters are shown at the bottom of each picture. Two semisphere pits are close to each other and sometimes they are overlapped. On the ridge between the two pits, a smaller semisphere pit is usually found. Here, such a phenomenon is called "pits chain". The "pits chain" has such a specific shape that it is considered to be formed sequentially, not randomly. It indicates that the existed erosion pits have some effect on the pits formed later, and the whole erosion process is not a probability event.

To study the development of the erosion pits, the same area on the grinded sample surface was observed at different experimental times. In this experiment, the same area on the same sample surface was observed after 2 min, 2 h and 24 h, respectively. The pictures of the damaged surface are shown in figure 3.

In figure 3(a), some semisphere and needle-like pits appear on the surface after the short experimental time, but most of the pits are not in contact with each other, and they disperse on the surface randomly. After 2 h, some new pits appear near the existed pits and they are sometimes in contact with each other to form the "pits chain". After 24 h, the sample surface is severely damaged by the cavitation erosion. The surface is fully occupied by the connected and overlapped erosion pits. There are still some pits with clear semisphere edges on the surface, which indicates that the cavitation erosion would continue its process vertically after it destroys the original surface.

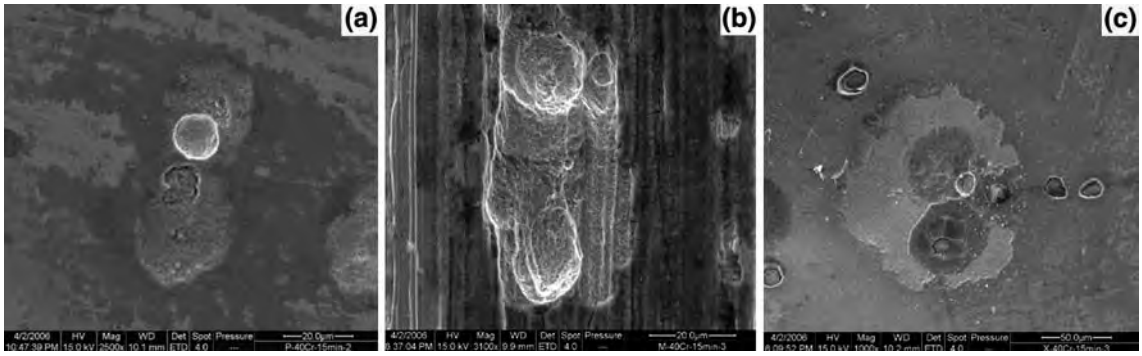

Figure 2. Three different surfaces observed under SEM after the experiment. (a) is the polished surface, (b) is the grinded surface, (c) is the milled surface.

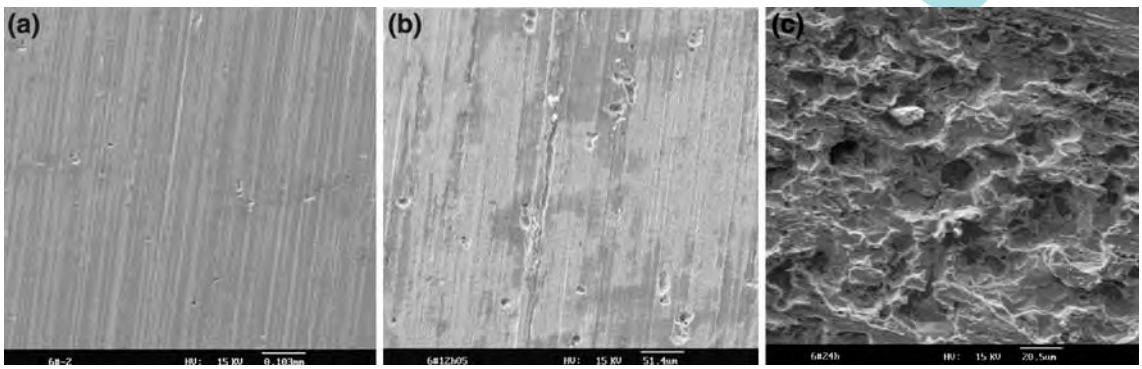

Figure 3. The development of the cavitation erosion on the grinded sample surface. (a) After 2 min (b) After 2 h (c) After 24 h.

3. Numerical analysis

3.1. Method and model

The experimental results suggest that the pits generated in early stages affect the formations of the pits in later stages. An obvious reason for this result is that the existence of a pit on the surface would change the flow field around it, which may provide a suitable environment for the collapse of a bubble. The changes of the flow conditions were simulated, and all the calculations were performed using the commercial CFD software named FLUENT. Some basic conditions and assumptions are adopted here as follows.

(1) The shape of a pit is treated as a cosine curve, the wavelength is 10 μm and the amplitude is 1 μm.
(2) The fluid is water, which is a Newtonian fluid with constant viscosity.
(3) The thermal effect is not included in this calculation. The ''pits chain'' is thought to be formed sequentially, so two different geometry models of the calculating domain are used and shown in figure 4. The difference between the two models is the stationary solid wall A in figure 4. The continuous line represents the model with only one pit on the solid surface, while the dotted line represents that there are two pits on the solid wall. The boundary conditions are defined as follows: A is the stationary wall, while the upper boundary C is a moving wall with the speed of 30 m/s; the left side D and right side B are treated as periodic boundaries. The boundaries B and D were divided into 120 grids with a grow factor of 1.05, boundaries A and C were divided into 60 grids, so the number of the grids was $120 \times 60 = 7{,}200$.

In FLUENT, a control-volume-based technique is used to convert the governing equations to algebraic equations that can be solved numerically, which is called the finite volume method. The continuity equation and momentum equation are adopted in the calculation, which are applicable for any continuous medium. In the calculation, the implicit formulation is used for the steady process; the pressure is solved using PRESTO! the pressure–velocity coupling equation is solved using PISO [10], and the momentum equation is solved using the second order upwind method. The residual definitions are used for judging convergence. This criterion requires that the residuals decrease to 10^{-6} for the continuity equation and velocity equation. In this calculation, the residuals both reach the convergence criteria and almost keep constant after 12,500 iteration steps, which indicates that the numerical process is converged.

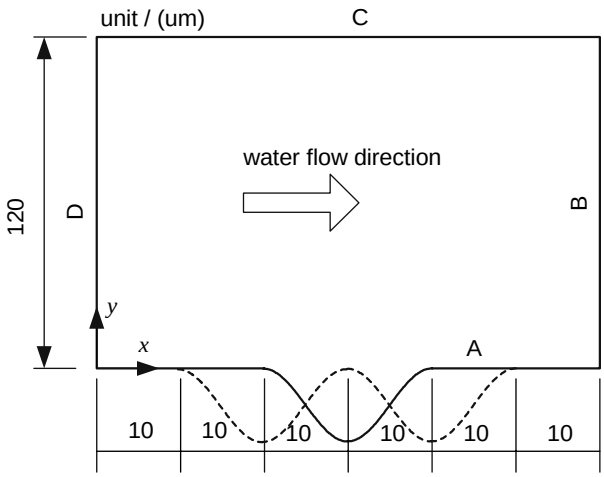

Figure 4. Geometry model of the calculating domain and its boundaries.

3.2. Numerical results

It has been recognized that the collapse of a bubble is greatly related to the perturbation of the environment pressure [6, 11]. When a pit is generated on the solid wall, the pressure on the pit fluctuates. Usually, the pressure decreases on the trailing edge of a pit, while it increases on the rising edge. The calculated pressures on the solid wall with one and two pits are shown in figure 5(a) and (b), respectively. In each figure, a low pressure domain and a high-pressure domain appear alternatively along the flow direction. The existence of a pit causes a sinusoidal-like variation of the pressure, which is represented in figure 5(c). When a bubble is assumed to pass the pit, it goes into the low-pressure domain first. The bubble would expand but not collapse in this domain. However, the bubble later goes into the high-pressure domain before it moves away from the pit. In the high-pressure domain, the bubble would be compressed or even collapse. Therefore, the bubble experiences an expansion–compression process when it passes a pit near the wall.

If the pressure fluctuation can be seen as a perturbation added on a stable bubble with an ideal spherical shape, it should be solved when the perturbation is strong enough to break the stability of the bubble and causes it to collapse before it moves out of the pit. Here, the perturbation theory on a spherical bubble was adopted to solve the problem [12]. The equation describing the stability of a bubble under perturbation is shown as equation (1) [12].

$$z(1-z)\frac{d^2a_n}{dz^2}+\left(\frac{1}{3}-\frac{5}{6}z\right)\frac{da_n}{dz}-\frac{n-1}{6}a_n=0 \qquad (1)$$

Where $z = R/R_0$, R is the radius of a bubble and R_0 is the initial radius of the bubble; a_n is the amplitude of the perturbation on the bubble's wall; n is the order of the Legendre function. The initial perturbation velocity u_0 is represented by a nondimensional parameter l_0 shown in equation (2) [12], where p is the pressure difference on the bubble, and ρ is the fluid density.

$$l_0 = u_0 R_0 \Big/ \sqrt{2p/3\rho} \qquad (2)$$

After solving equation (1) with the initial condition $n = 6$, $l_0/a_0 = 0$ and $l_0/a_0 = 1/3$, the perturbation variation during the bubble's compress process is shown in figure 6 (the detailed solving process is referred to [13] and [12]). The curve shows that the stability of the bubble is related to the compression ratio R/R_0. When the ratio is larger than 0.2, the perturbation amplitude is quite small, so the bubble keeps stable; but when the

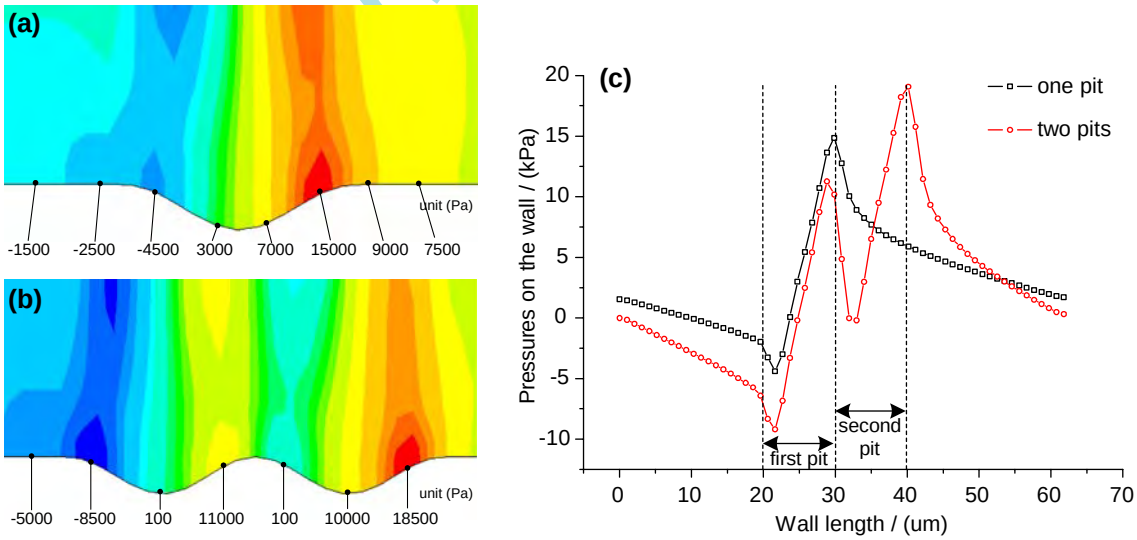

Figure 5. Numerical results of pressures on the solid surface with pits on it. (a) one pit on the surface, (b) two pits on the surface, (c) pressure distribution on the solid wall.

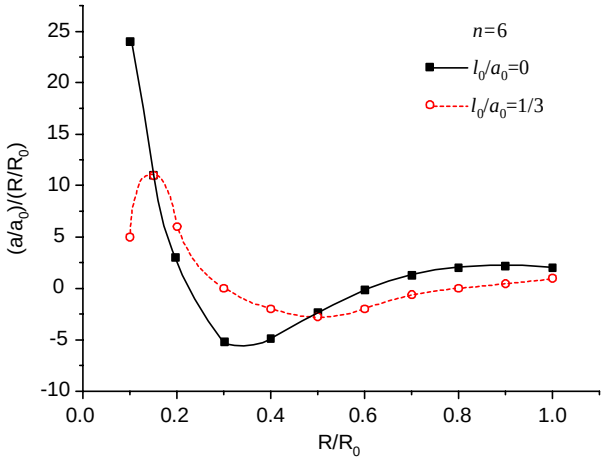

Figure 6. Perturbation variation on the bubble during the bubble's compress process.

ratio is less than 0.2, the perturbation amplitude grows rapidly. It means that the stability of the bubble is broken, and the bubble collapses at last.

So the compress ratio is a key parameter to determine the stability of the bubble under the perturbation. Usually, the compress process is very rapid, and the compress ratio of a bubble can be calculated as equation (3) under the static flow field condition [14].

$$\frac{p}{p_0} = 1 + \left[\left(\frac{R_0}{R}\right)^3 - 4\right]^{4/3} \Big/ \left\{4^{4/3}\left[\left(\frac{R_0}{R}\right)^3 - 4\right]^{1/3}\right\} \quad (3)$$

The high-pressure value is acquired from figure 5. The maximum pressure p is 15,000 Pa and the initial pressure in the bubble p_0 is 270 Pa, then the compression ratio R/R_0 is approximately 0.14. According to figure 6, the bubble would be unstable and it would collapse. The compression time can be calculated according to equation (4) [14]. With the parameter $R_0 = 10\mu$m, $p_0 = 270$ Pa, the compression time is 7.19 μs. The compression process is so rapid that the bubble will collapse before it moves away from the pit. (The collapse time can be omitted compared with the compression time).

$$t = R_0\sqrt{\frac{\rho}{6p_0}} \cdot \frac{\Gamma(5/6)\Gamma(1/2)}{\Gamma(4/3)} = 0.915R_0\sqrt{\frac{\rho}{6p_0}} \quad (4)$$

Here, the wavy surface profile is considered to cause a pressure fluctuation, and the bubble is compressed and will collapse at last. The generally accepted mechanism of cavitation erosion is the shock waves and micro jets generated at the moment of bubble collapse when a bubble is close to a solid surface [15]. Moreover, the experimental study [16] shows that the micro jet is the main reason for the erosion when the bubble is within a certain distance from the solid wall, while the shock wave is the main reason for the erosion when the bubble is outside the distance. The collapsing pressure caused by the micro jets can be calculated using the traditional numerical method given by Plesset [11]. The value of the parameters used in the calculation is same as those used in equation (3). As the calculation results, the distance H from the bottom of the bubble to the solid surface and the velocity V of the jet stream generated at the moment of bubble collapsing are listed in Table 2. Considering the water hammer effect represented by equation (5) [11], the pressure caused by the water hammer effect changes from 50.7 MPa to 1132.5 MPa when the distance changes from 50 μm to 1 μm. It is known that the yield strength of 40Cr steel is about 800 MPa, so the micro jet stream can destroy the surface when the bubble is very near the solid surface. In the equation, the L and s subscripts refer to the liquid and the solid, respectively.

Table 2.
Velocities of the jet stream under different distance H.

H (μm)	V (m/s)
100	2.5
50	33.8
10	180
1	755

$$p_{WH} = \rho_L c_L v\left(\frac{\rho_s c_s}{\rho_L c_L + \rho_s c_s}\right) \quad (5)$$

The results shown in Table 2 also indicate that the micro jet will not have obvious effect on the solid surface because the velocity of the jet stream decreases rapidly in the water as the distance increases. Under that condition, the shock waves will replace the micro jets to cause the erosion pits when the distance is outside the coverage of jet stream. Numerical results [17] show that the pressure caused by shock waves reach the order of 10^3MPa, which can damage steel surfaces. Experimental results [16] also support the viewpoint.

Based on the numerical analyses, the experiment phenomenon "pits chain" can be explained. Firstly, a bubble collapses near the smooth solid surface and causes a pit on the surface, which can be seen as a probability event. Then, a pressure fluctuation is generated on the pit surface. When a bubble is passing the pit near the solid wall, it travels through the low-pressure domain first and then goes into the high-pressure domain. If the pressure were high enough, the bubble would collapse on the rising edge before it moves out of the high-pressure domain. If there are two pits on the surface, two high-pressure domains will be formed. The pressure in the first domain is slightly lower than that in the second one. So the bubble would collapse with great

probability in the first high-pressure domain. A new pit is formed then on the ridge between the two contact pits. In brief, the pressure fluctuation caused by the pits on the solid surface is the reason for the formation of "pits chain".

3.3. Discussions

The whole erosion process can also be analyzed by the surface roughness related unstable bubble theory as it has been applied to explain the typical erosion result "pits chain". Based on the mechanism that the erosion pit is mainly caused by the bubble collapse near a solid wall, the development of the cavitation erosion on solid surface is divided into four different stages, which are described by the different curves in figure 7.

In stage 1, the formation of the first pit on the solid surface is considered as a probability event because the surface condition is all the same at any place. In this stage, the surface is characterized by the scattered needle-like pits, which can be obviously found in the SEM picture figure 3(a). In stage 2, the pit formed in stage 1 causes the pressure fluctuation and the collapse of the bubble when the bubble is passing the rising edge of the pit. Then, a new pit is formed on the surface just behind the existed pit. In stage 3, a bubble would experience two high-pressure domains before it moves away from the second pit. If the pressure were high enough in the first domain, the bubble would collapse, and form a new pit on the ridge between the two existed pits. Then the "pits chain" appears on the surface. If the bubble has past the first domain, it will go into the second domain but it usually does not collapse yet because the pressure in the second domain is almost the same as that in the first domain, so the bubble will move out of the pits domain. In stages 2 and 3, the surface is characterized by the "pits chains". Figure 3(b) shows the results of the two stages. The number of connected pits pairs is increased and some "pits chains" appear on the surface. In stage 4, the "pits chain" becomes a larger pit with a rough bottom. When the asperity on the rough bottom is high enough to generate high-pressure domain, the bubble collapses on the bottom, which makes the erosion develop vertically. Besides, if the asperity is not high enough, the "pits chain" is still seen as a pit, and the pits expansion process is the same as stage 2. Then, the erosion develops horizontally. Erosion development in this stage explains the erosion result shown in figure 3(c). It is found that the original surface is occupied by the erosion pits, and the pits are superposition to form a new surface. It indicates that the erosion expands horizontally. On the other hand, some hemispherical pits with clear edges are observed on the new-formed surface, and it suggests that the erosion should develop vertically. It should be noted here that at least one condition should be satisfied to generate the "pits chain", that is the bubble should be close to the wall. Only under this condition, the fluctuated pressure can affect the stability of a bubble effectively and cause it to collapse, and furthermore, the jet stream generated at the moment of collapse can damage the surface [11]. So not all the needle-like pits can develop to the "pits chain", while the "pits chain" is a typical process during the cavitation erosion process when the cavitation is strenuous.

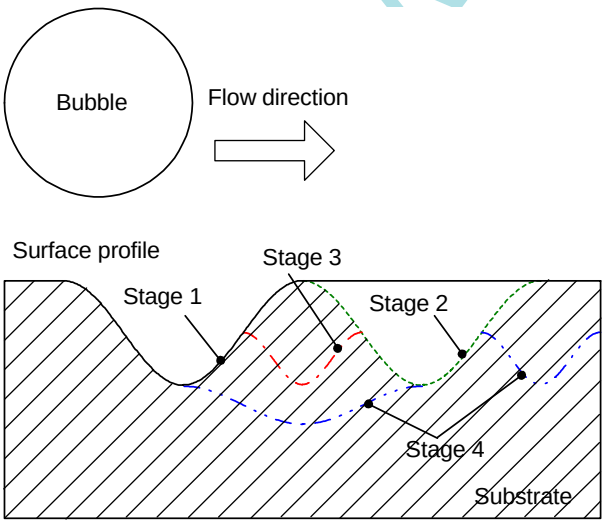

Figure 7. Four different stages of the cavitation erosion development.

4. Conclusions

A cavitation experiment was performed on three different sample surfaces to investigate the development of the cavitation erosion. Under the condition that the erosion pits are mainly caused by the collapse of bubbles near the solid wall, some conclusions are drawn as follows:

(1) A typical phenomenon of "pits chain" was found on the sample surfaces after the 15-minute experiment. "Pits chain" consists of two contact pits and a smaller pit on the ridge between them. According to the numerical analyses, it is believed that an early-formed pit causes a pressure perturbation on the pit surface, and the bubble would collapse at the rising edge of the existed pit under the pressure perturbation. Then the "pits chain" forms sequentially.

(2) In the experiment, the development of the cavitation erosion is divided into four stages. In stage 1, bubbles collapse randomly and scattered needle-like pits appear on the solid surface. In stages 2 and 3, bubbles collapse at the rising edge of the existed pits, and then the phenomenon of "pits chain" appears on the surface. In stage 4, erosion develops vertically and horizontally under the effect of the bubble collapse, and the surface is severely damaged by the erosion.

Acknowledgments

The authors would like to thank *Ms. Jiang nana* and *Mr. Qin Li* (Tsinghua University) for their help in preparing the experiment. This work is supported by the *Research Fund for the Doctoral Program of Higher Education*(No. 20030003026), *NSFC Project* (No. 50505020), and *NSFC Project* (No. 50475018).

References

[1] F.G. Hammitt, *Cavitation and multiphase flow phenomena* (McGraw-Hill Inc., USA, 1980).
[2] C.L. Kling, A high speed photographic study of cavitation bubble collapse, Ph.D. thesis, University of Michigan, 1970.
[3] N.D. Shutler and R.B. Mesler, Transaction of ASME, J. Basic Engr. 87 (1965) 511.
[4] P.V. Marques and E.T. Roseana, Mater. Charact. 41 (1998) 193.
[5] Iwai Yoshiro and Li. Shengcai, Wear 254 (2003) 1.
[6] G. Birkhoff, Q. Appl. Math. 25 (1954).
[7] K.A. Mørch, J. Fluids Eng. 122 (2000) 494.
[8] M. Pohl and J. Stella, Wear 252 (2002) 501.
[9] S.F. Jones, G.M. Evans and K.P. Galvin, Adv. Colloid Interface Sci. 80 (1999) 27.
[10] FLUENT User's guide handbook, Release version: 6.1.18, 1998 Fluent Inc.
[11] M.S. Plesset and R.B. Chapman, J. Fluid Mech. 47 (1971) 283.
[12] M.S. Plesset, T.P. Mitchell, Q. Appl. Mathematics 13 (1956).
[13] J.T. Huang, *Theory and Application of Cavitation and Cavitation Erosion* (Tsinghua Univ. Press, 1991) pp. 50–51. In Chinese.
[14] J.T. Huang, *Theory and Application of Cavitation and Cavitation Erosion* (Tsinghua Univ. Press, 1991) pp. 24–25. In Chinese.
[15] F.G. Hammitt, Mechanical cavitation damage phenomena and corrosion fatigue, UMICH report, No. 03371–7-T, University of Michigan, 1971.
[16] A. Shima, K. Takayama and Y. Tomita, Mechanisms of the bubble collapse near a solid wall and the induced impact pressure generation, Rep. Inst. High Speed Mech., Tohoku Univ., Vol. 48 (1984).
[17] R. Hickling and M.S. Plesset, Phys. Fluids 7 (1964) 7.